HIGH-POWER SPATIALLY EXTENDED FREE-ELECTRON MASERS WITH THREE-DIMENSIONAL DISTRIBUTED FEEDBACK

N. Yu. Peskov,[1,2] * **E. D. Egorova,**[1,2] **N. S. Ginzburg,**[1,2]
A. S. Sergeev,[1] **A. V. Arzhannikov,**[2] and
S. L. Sinitsky [2]

UDC 621.385

We study the possibility of using Bragg resonators that implement a three-dimensional distributed feedback mechanism ensuring synchronization of radiation and mode selection under conditions of substantial oversize in three spatial coordinates. To describe the electron–wave interaction in devices of this type, a three-dimensional spatiotemporal averaged model was developed within the framework of the coupled wave approach. On this basis, a planar free-electron maser (FEM) driven by a full-scale electron beam of a sheet configuration with a particle energy of 1 MeV, a current of up to 140 kA, and a cross section of about 1×140 cm, which is formed using a high-current accelerating complex U-2 (BINP RAS), was simulated. The possibility of achieving a stable narrow-band oscillation regime in FEMs with a multi-gigawatt power level in the W band with transverse sizes of the proposed resonators from tens to hundreds of radiation wavelengths is demonstrated.

1. INTRODUCTION

The creation of high-power (0.1–1000 MW) sources of coherent electromagnetic radiation operating in the short-wavelength part of the millimeter and submillimeter wavelength ranges is one of the key tasks of modern high-power electronics. The need for such sources is due to a wide range of fundamental problems, including the creation of electron–cyclotron plasma systems, efficient compact X-ray free electron lasers, and new high-gradient acceleration schemes. Such sources are also widely in-demand at present in the field of engineering and technical applications related to the development of new technologies, the creation of systems for visualizing hidden objects and counter terrorism, the development of radar systems with high temporal and spatial resolution and other modern radio-engineering systems. By now, in a long-pulse regime (from microseconds to continuous-wave mode) the highest radiation power in the indicated ranges (from a few megawatts in the subterahertz range up to tens of kilowatts in the terahertz range) was obtained using gyrotrons [1–5]. A radical increase in pulsed radiation power up to sub-gigawatt/gigawatt levels in these ranges can be achieved in relativistic oscillators based on intense electron beams with kiloampere level currents.

The concept of high-power spatially extended relativistic free-electrons masers (FEMs) has been developed over a number of years in collaboration of the A. V. Gaponov-Grekhov Institute of Applied Physics of the Russian Academy of Sciences (IAP RAS, Nizhny Novgorod) with the G. I. Budker Institute of Nuclear
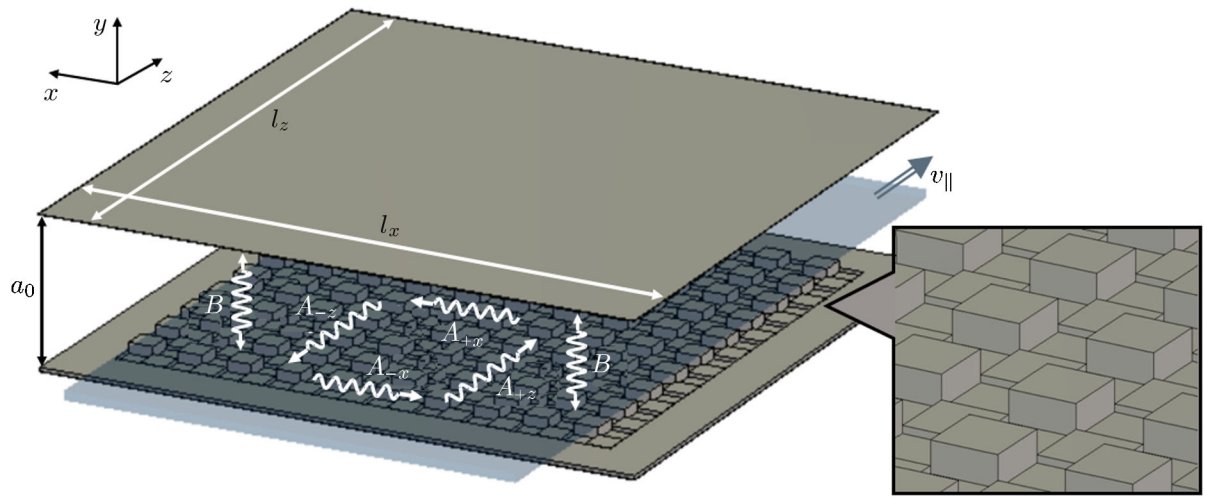
---

* peskov@ipfran.ru

Fig. 1. Diagram of the interaction space of the FEM with a Bragg resonator, which provides three-dimensional distributed feedback. A sheet electron beam moving in the $+z$ direction and partial wave flows forming a feedback loop are shown. The leader shows the corrugation structure of the plates in a resonator of this type.

Physics of the Siberian Branch of the Russian Academy of Sciences (BINP RAS, Novosibirsk). The main idea is transition to a sheet configuration of high-current relativistic electron beams (REBs) and planar geometry of the interaction space, which ensures an increase in the integral power of the output radiation due to an increase in one of the transverse sizes of the oscillator while maintaining current densities and electromagnetic flows. The experimental basis of the concept being developed is sheet REBs generated on the basis of various accelerator facilities at the BINP RAS [6]:

1) the beam for modeling experiments with a particle energy of 1 MeV, a current of 10 kA, a duration of 3 μs, a cross section of 0.3×20 cm, and energy content of the order of 10 kJ, generated by the U-3 accelerator of the ELMI setup;

2) the full-scale beam with a particle energy of 1 MeV, a current of 140 kA, a duration of 10 μs, a cross section of 1×140 cm, and an energy content of up to 0.4 MJ, generated by the U-2 accelerator.

In the course of research performed on the basis of the U-3 accelerator of the ELMI setup, a W-band FEM (operating frequency 75 GHz) was created, which for transverse cavity sizes of about 2.5×50 radiation wavelengths λ showed a stable narrow-band oscillation regime with output radiation power at a level of the order of 100 MW [7]. This power is record-breaking for this class of oscillators. Synchronization of radiation of a sheet REB in this FEM oscillator was achieved by using a two-dimensional distributed feedback mechanism, which is implemented in two-dimensional periodic Bragg structures due to the emerging additional transverse flows of electromagnetic energy. These flows provide the development of the system along the "wide" transverse coordinate (the x coordinate directed parallel to the plates of the planar system, see Fig. 1) [8, 9].

A further dramatic increase in FEM power can be achieved by using a full-scale sheet REB formed by the U-2 accelerator. However, the gap of a planar system required to transport this beam through the interaction space (taking into account the actual beam width and amplitude of its bounce oscillations in the undulator) is 3–4 cm, i. e., about 10λ in the frequency range discussed. Under these conditions, the use of Bragg structures that implement two-dimensional distributed feedback becomes ineffective, because they lose their selective properties when increasing the size along the second, "narrow" transverse coordinate (the y coordinate directed along the gap of a planar system in Fig. 1).

In this regard, to create a super-powerful relativistic maser of planar geometry based on a spatially extended sheet REB, the development of an electrodynamic system capable of providing effective mode selection under conditions of high oversize along both transverse coordinates becomes the key problem. To solve this problem, the authors of [10] proposed the use of a new type of Bragg structures that implement

a feedback mechanism, which can be called three-dimensional. In addition to the wave flows generated by two-dimensional structures, quasi-cutoff waves (similar to advanced Bragg structures [11, 12]), which are trapped between the plates of a planar resonator, are involved in the feedback loop of these structures. These waves permit effective mode selection and extension of the system in the second transverse direction. Thus, when selection methods used in two-dimensional and modified analogues are combined in structures of a new type, it becomes possible to provide for selection with respect to both transverse mode indices. High selective properties of three-dimensional Bragg structures were confirmed by simulation using the CST Microwave Studio code [10].

2. MODEL AND BASIC EQUATIONS

The Bragg resonator based on the mechanism of three-dimensional distributed feedback (Fig. 1) is a section of a planar waveguide, the walls of which are corrugated according to the law

$$a = a_{2D} \cos(\bar{h}x) \cos(\bar{h}z) + a_{1D}[\cos(\bar{h}x) + \cos(\bar{h}z)]. \tag{1}$$

When the Bragg resonance condition

$$\bar{h} \approx h \tag{2}$$

is fulfilled, this corrugation ensures the scattering of wave flows propagating in three mutually perpendicular directions. The corresponding electric field at a point with coordinates x, y, and z at the time moment t is given by

$$\mathbf{E} = \text{Re}\left\{[A_{+z}\exp(-ihz) + A_{-z}\exp(ihz) + A_{+x}\exp(-ihx) + A_{-x}\exp(ihx)]\mathbf{E}_A\exp(i\omega t) \right.$$
$$\left. + B\mathbf{E}_B\exp(i\omega t)\right\}. \tag{3}$$

The first term in Eq. (1) (similar to the two-dimensional Bragg structure [8, 9]) is responsible for mutual scattering of wave flows $A_{\pm z}$ and $A_{\pm x}$, which propagate in the $\pm z$ and $\pm x$ directions, respectively. The second term (similar to advanced Bragg structures [11, 12]) ensures scattering of these waves into a quasi-critical wave B, which (according to the Brillouin concept) can be interpreted as a standing wave in the y direction trapped between the plates of a planar waveguide. Here, ω is the radiation frequency, $\bar{h} = 2\pi/d$, d is the corrugation period, a_{1D} and a_{2D} are the amplitudes of the corresponding components (spatial harmonics) of corrugation, $A_{\pm z;\pm x}$ and B are the slowly varying amplitudes of partial waves and $\mathbf{E}_{A;B}(y)$ are functions describing the transverse (along the y axis) structure of these waves, which coincide with the eigenmodes of an unperturbed planar waveguide. For definiteness, we assume that the waves $A_{\pm z;\pm x}$ belong to the lower TEM type. In this case, the wave B belongs to one of TM$_p$ waves of a planar waveguide. Under conditions of significant oversize (i. e., when $a_0 \gg \lambda$), this wave has a high transverse index $p \gg 1$ and, accordingly, a large number of variations along the y coordinate directed along the gap between plates.

Within the framework of the coupled wave method [13–15], the process of mutual scattering of partial waves (3) by a corrugated surface (1) can be described by equations for slow amplitudes $A_{\pm z;\pm x}(t, x, z)$ and $B(t, x, z)$. To simulate the dynamics of the FEM with three-dimensional Bragg resonator, we assume that the condition of undulatory synchronism

$$\omega - hv_\parallel \approx \Omega_b \tag{4}$$

between the co-propagating wave A_{+z} and the electrons moving along the $+z$ direction with velocity $v_\parallel = \beta_\parallel c$ (c is the speed of light in empty space) and oscillating in the undulator field with bounce frequency $\Omega_b = h_u v_\parallel$ ($h_u = 2\pi/d_u$, d_u is the undulator period) is fulfilled. It is assumed that the electron beam is focused by a uniform guiding magnetic field. Interaction of a sheet REB with a synchronous wave A_{+z} taking into account the mutual scattering of partial wave flows (3) by corrugation (1) can be described by the equations (cf. [8, 9])

$$\frac{\partial \hat{A}_{+z}}{\partial Z} + \frac{\partial \hat{A}_{+z}}{\partial \tau} + i\alpha_{2D}(\hat{A}_{+x} + \hat{A}_{-x}) + i\alpha_{1D}\hat{B} = J\,F(X), \tag{5a}$$

523

$$\frac{\partial \hat{A}_{-z}}{\partial Z} - \frac{\partial \hat{A}_{-z}}{\partial \tau} - i\alpha_{2D}(\hat{A}_{+x} + \hat{A}_{-x}) - i\alpha_{1D}\hat{B} = 0, \tag{5b}$$

$$\frac{\partial \hat{A}_{+x}}{\partial X} + \frac{\partial \hat{A}_{+x}}{\partial \tau} + i\alpha_{2D}(\hat{A}_{+z} + \hat{A}_{-z}) + i\alpha_{1D}\hat{B} = 0, \tag{5c}$$

$$\frac{\partial \hat{A}_{-x}}{\partial X} - \frac{\partial \hat{A}_{-x}}{\partial \tau} - i\alpha_{2D}(\hat{A}_{+z} + \hat{A}_{-z}) - i\alpha_{1D}\hat{B} = 0, \tag{5d}$$

$$\frac{iC}{2}\frac{\partial^2 \hat{B}}{\partial Z^2} + \frac{\partial \hat{B}}{\partial \tau} + \sigma\hat{B} + i\alpha_{1D}(\hat{A}_{+z} + \hat{A}_{-z}) + i\alpha_{1D}(\hat{A}_{+x} + \hat{A}_{-x}) = 0. \tag{5e}$$

The amplitude of the HF electron current in Eq. (5a)

$$J \approx \frac{1}{\pi}\int\limits_0^{2\pi} \exp(-i\theta)\,\mathrm{d}\theta_0$$

is determined from averaged equations of electron motion, which in regimes far from the cyclotron resonance can be represented in the form [16]

$$\left(\frac{\partial}{\partial Z} + \beta_\parallel^{-1}\frac{\partial}{\partial \tau}\right)^2 \theta = \mathrm{Re}\,[\hat{A}_{+z}\exp(i\theta)]. \tag{6}$$

Here, we used the following normalized variables and parameters: $\tau = C\bar{\omega}t$,

$$\begin{pmatrix} X \\ Z \end{pmatrix} = C\bar{h}\begin{pmatrix} x \\ z \end{pmatrix}, \qquad \begin{pmatrix} \hat{A}_{\pm z;\pm x} \\ \hat{B} \end{pmatrix} = \frac{eK\mu}{mc\bar{\omega}\gamma_0 C^2}\begin{pmatrix} A_{\pm z;\pm x}//\sqrt{N_A} \\ B/\sqrt{N_B} \end{pmatrix},$$

$\bar{\omega} = \bar{h}c$ is the frequency of exact Bragg resonance, which is chosen as the carrier frequency, θ is the electron phase relative to the synchronous wave, e is the elementary charge, m is the electron rest mass, γ_0 is the initial Lorentz factor,

$$C = \frac{eI_0}{mc^3}\frac{\lambda^2\mu K^2}{2\pi\gamma_0 a_0}$$

is the gain (Pierce) parameter, I_0 is the linear (over the cross section) beam current, $F(x)$ is a function describing the distribution of the electron flux density over the "extended" transverse coordinate x, N_A and N_B are the norms of the corresponding waves, $\sigma = s/(Ca_0)$ is the parameter characterizing ohmic losses in the resonator, and s is the skin layer thickness. The analysis shows that taking into account ohmic losses is fundamentally important for describing the quasi-critical wave B (see (5e)), while in Eqs. (5a)–(5d) for paraxial waves $A_{\pm z;\pm x}$ they can be neglected (similar to resonators of two-dimensional and advanced types [9, 11]).

The wave coupling coefficients in the case of corrugation of both plates are

$$\alpha_{2D} = \frac{a_{2D}}{4C\bar{h}a_0}, \qquad \alpha_{1D} = \frac{a_{1D}}{\sqrt{2}\,C\bar{h}a_0}$$

for two-dimensional [8, 9] and advanced [11, 12] Bragg scattering, respectively.

In the considered case of a sheet configuration of the electron beam and planar undulator geometry, the inertial bunching parameter μ and the electron–wave coupling coefficient K in regimes far from the cyclotron resonance are determined by the relations [16]

$$\mu = \gamma_0^{-2} + \frac{\alpha_u^2(1+q^2)}{4\gamma_0^2(1-q^2)^2}, \qquad K = \frac{\alpha_u q}{2\gamma_0(1-q^2)}, \tag{7}$$

where $\alpha_u = eH_u/(h_u mc^2)$, $q = \omega_{H0}/(\gamma_0\Omega_b)$, $\omega_{H0} = eH_0/(mc)$ is the nonrelativistic gyrofrequency, and H_u

and H_0 are the undulator and guiding magnetic fields, respectively. It should be noted that according to the previous analysis [9, 16], such regimes are advantageous in terms of quality of the formation of magnetically guided REBs in the undulator and thus achieving high efficiency of electron–wave interaction in the FEM.

In the normalizations used, the integral efficiency is

$$\eta = \frac{C}{\mu(1 - \gamma_0^{-1})}\hat{\eta}, \qquad \hat{\eta} = \frac{1}{2\pi L_x} \int\limits_0^{L_x} \mathrm{d}X \int\limits_0^{2\pi} \left. \left(\frac{\partial\theta}{\partial Z} + \Delta \right) \right|_{Z=L_z} \mathrm{d}\theta_0. \tag{8}$$

At the boundaries of the resonator for paraxial partial waves we assume perfect consistency and absence of electromagnetic flows from the outside, which is described by boundary conditions of the form

$$\hat{A}_{+z} \mid_{Z=0} = 0, \tag{9a}$$
$$\hat{A}_{-z} \mid_{Z=L_z} = 0, \tag{9b}$$
$$\hat{A}_{+x} \mid_{X=0} = 0, \tag{9c}$$
$$\hat{A}_{-x} \mid_{X=L_x} = 0, \tag{9d}$$

where $L_{z;x} = \bar{h}l_{z;x}$ are the normalized length and width of the resonator, respectively. Boundary conditions for a quasi-cutoff wave (see [17] for more details)

$$\left[\hat{B} - \sqrt{\frac{C}{2\pi i}} \int\limits_0^\tau \frac{\exp[-\sigma(\tau - \tau')]}{\sqrt{\tau - \tau'}} \frac{\partial\hat{B}(\tau')}{\partial Z} \mathrm{d}\tau' \right] \Bigg|_{Z=0} = 0, \tag{9e}$$

$$\left[\hat{B} + \sqrt{\frac{C}{2\pi i}} \int\limits_0^\tau \frac{\exp[-\sigma(\tau - \tau')]}{\sqrt{\tau - \tau'}} \frac{\partial\hat{B}(\tau')}{\partial Z} \mathrm{d}\tau' \right] \Bigg|_{Z=L_z} = 0, \tag{9f}$$

also correspond to the absence of reflections and its free emission from the resonator.

Boundary conditions for an initially unmodulated monoenergetic electron flux has the form

$$\theta \mid_{Z=0} = \theta_0 \in [0; 2\pi), \qquad \left. \left(\frac{\partial}{\partial Z} + \beta_\parallel^{-1} \frac{\partial}{\partial \tau} \right) \theta \right|_{Z=0} = \Delta, \tag{10}$$

where $\Delta = (\bar{\omega} - \bar{h}c - h_\mathrm{u}c)/(\bar{\omega}C)$ is the initial mismatch of the electron–wave synchronism at the carrier frequency.

3. SIMULATION RESULTS

The simulation was carried out with sheet REB parameters close to the parameters of the beam formed by the U-2 accelerator: electron energy about 1 MeV, beam linear current 1 kA/cm, and beam cross section 1×140 cm. To build-up bounce oscillations of the electrons, it is proposed to use a planar undulator with period $d_\mathrm{u} = 4$ cm and amplitude $H_\mathrm{u} \approx 1$ kOe of the transverse undulator field on the beam trajectory for focusing and transporting the REB, namely, use a uniform guiding field with the strength $H_0 \approx 12$–15 kOe (a magnetic system with similar parameters was employed in the experiments described above [7]). With the indicated parameters, the operating transverse velocity of particles in the undulator is approximately 0.25 c.

The three-dimensional Bragg resonator was designed to operate in the W-band frequency range. The frequency of the fundamental (operating) mode was about 75 GHz. Transverse sizes of the resonator were chosen so as to transport the beam formed by the U-2 accelerator in the FEM interaction space and ensure effective electron–wave interaction. Thus, the width of the system was taken equal to $l_x = 150$ cm (which in the W-band is 350–400 radiation wavelengths) and the distance between the plates (gap) was $a_0 = 4$ cm
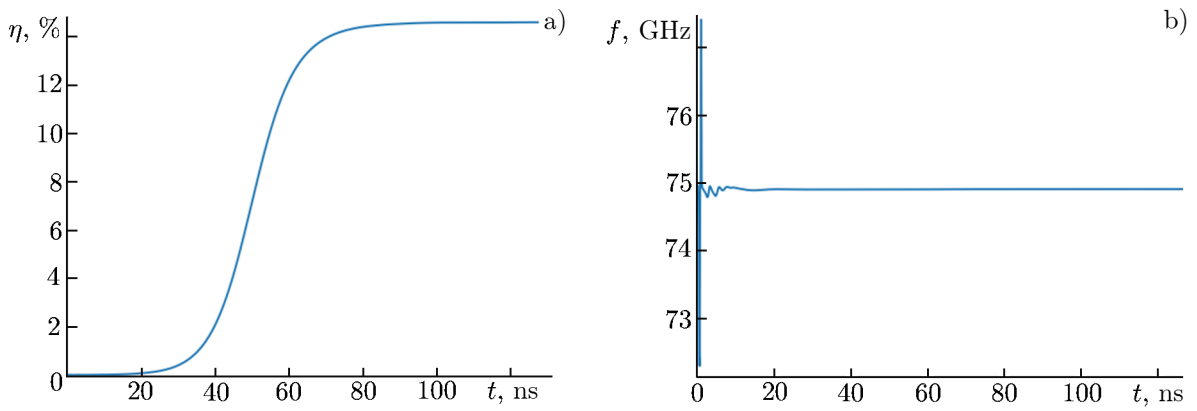
Fig. 2. Results of modeling a planar FEM with three-dimensional distributed feedback based on the U-2 accelerator. Onset of a stationary oscillation regime with optimal parameters, namely, the dependence of the electron efficiency η (a) and "current" radiation frequency f (b) on time.
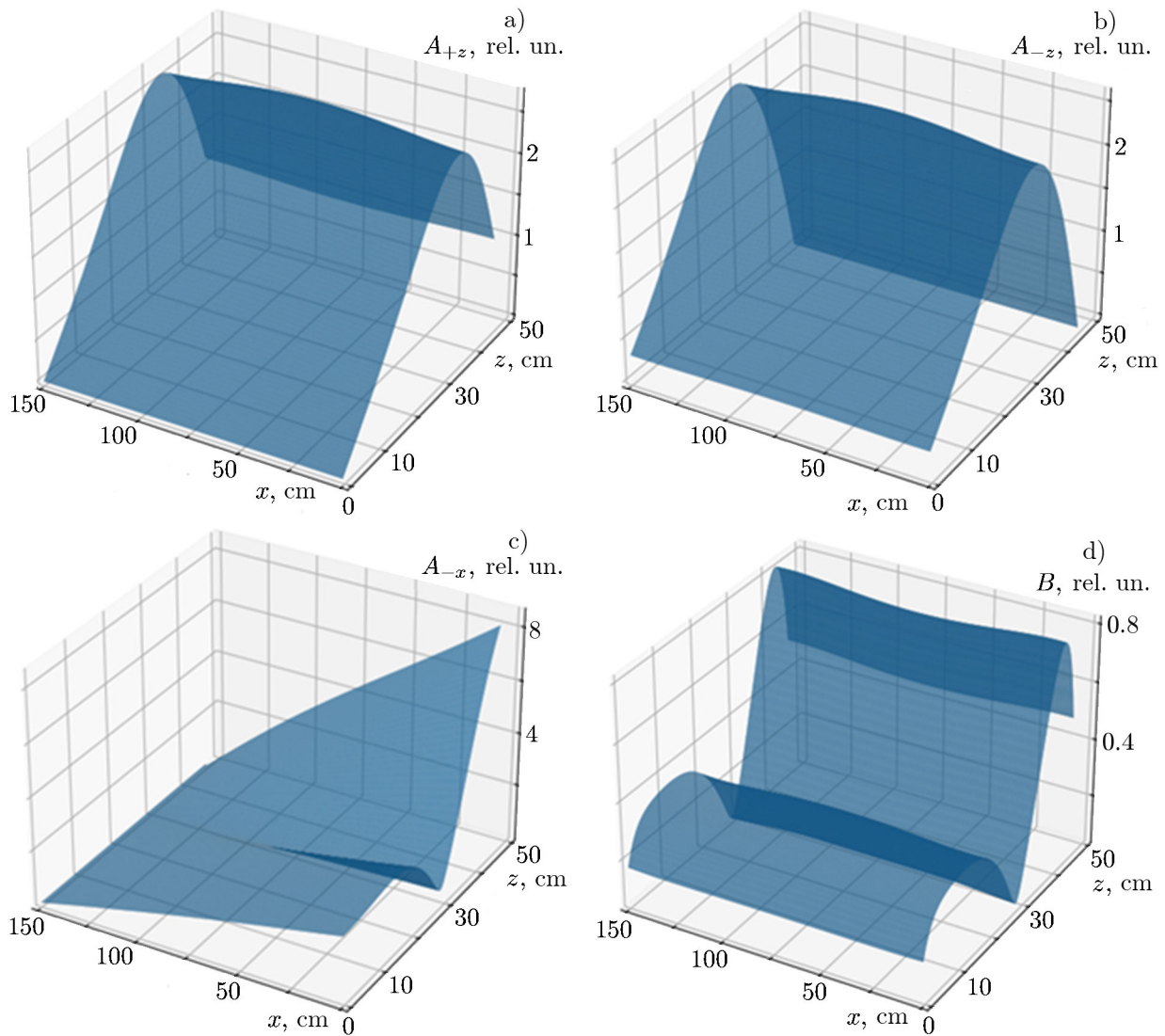

Fig. 3. Structures of the fields of partial waves in a stationary oscillation regime with optimal parameters: co-propagating wave A_{+z} interacting with electrons (a), counter-propagating feedback wave A_{-z} (b), transversely propagating "synchronization" wave A_{-x} (c), and quasi-cutoff wave B (d).

(i.e., about 10λ). It should also be noted that in modeling, the corrugation parameters ensured equality of the Bragg frequency and the cutoff frequency of the wave B.

The results of modeling the spatiotemporal dynamics of a planar FEM oscillator based on a three-dimensional Bragg resonator are presented in Figs. 2–4. Simulations show that using a Bragg resonator for effective mode selection in three spatial coordinates ensures, with optimal parameters, the onset of a stable stationary oscillation mode under conditions of the considered substantial oversize (Fig. 2a). In this case, the oscillation frequency in the steady state is close to the Bragg frequency (Fig. 2b), which corresponds to the excitation of the fundamental mode of a three-dimensional resonator. Structures of the fields of partial waves $A_{\pm x}$, $A_{\pm z}$, and B in the stationary regime (Fig. 3) are also close to the structures of the corresponding partial waves of the highest-Q mode of a three-dimensional Bragg resonator, found earlier within the framework of "cold" modeling [10].

Fig. 4. Dependence of the electron efficiency in steady state on the mismatch of undulator synchronism Δ. The blue curve shows the excitation area of the fundamental mode of a three-dimensional Bragg resonator and the brown curve shows the higher-order modes.

According to the simulation, the most effective electron–wave interaction is achieved for the interaction space (resonator) length $l_z \approx 50$–70 cm. Under these conditions, the synchronous partial wave A_{+z} has a fairly favorable longitudinal structure for efficient bunching and energy release of electrons, and its transverse distribution almost does not depend on the transverse coordinate x, providing identical interaction conditions for all fractions of the spatially developed sheet REB (see Fig. 3).

The maximum electron efficiency is achieved in the region of relatively large values of the negative mismatch of synchronism Δ. However, these regimes have an increased time of onset of self-oscillations. In the region of optimal parameters for a moderate mismatch of synchronism, the characteristic transition time is 50–70 ns, and the electron efficiency in steady state reaches 10–15%, which with a total (integral over the cross section) beam current of about 140 kA, corresponds to the output radiation power at a level of 10–20 GW. Herein, according to the modeling, ohmic losses for a cavity made of copper do not exceed 10% of the power emitted by the beam.

It should also be noted that with large positive detunings there was excitation of higher-order cavity modes (see Fig. 4). However, these modes have a less favorable spatial field structure for interaction with a sheet REB and, therefore, are characterized by a lower efficiency.

4. CONCLUSIONS AND DISCUSSION

Thus, theoretical analysis and computer modeling demonstrate high selective properties of spatially developed Bragg resonators that provide a three-dimensional distributed feedback mechanism. These resonators permit the selection of oscillations with an oversize parameter that reach values from tens to hundreds of wavelengths in all three spatial coordinates. The indicated transverse sizes exceed the well-known analogues both for relativistic oscillators [18] and high-power gyrotrons [1–5].

Within the framework of the developed spatiotemporal model of electron–wave interaction, we simulated the dynamics of a planar FEM with radiation synchronization based on three-dimensional distributed feedback. The possibility of creating a superhigh-power W-band oscillator based on the U-2 accelerator (BINP RAS), which forms an electron beam with a particle energy of 1 MeV, a current of 140 kA, a duration of 10 μs, and a cross section of 1×140 cm. According to the simulation, the use of a new type of resonator ensures stable narrowband oscillation in the FEM with a transverse oversize parameter reaching about 10×400. In this case, the electron efficiency can be 10–15%, which, with a total beam current, provides a record-breaking multi-gigawatt output power level for high-current microwave oscillators.
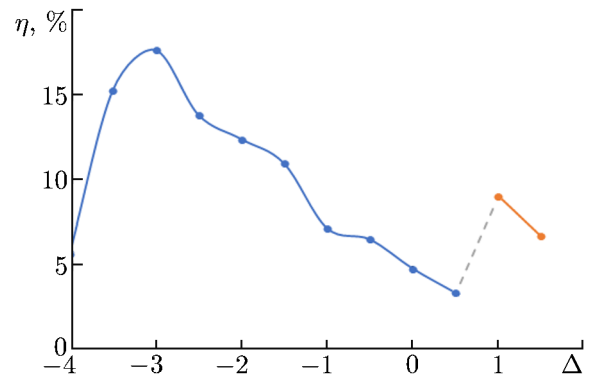
REFERENCES

1. A. G. Litvak, G. G. Denisov, and M. Yu. Glyavin, *IEEE J. Microwaves*, **1**, 260–268 (2021). https://doi.org/10.1109/JMW.2020.3030917

2. M. K. A. Thumm, G. G. Denisov, K. Sakamoto, and M. Q. Tran, *Nucl. Fusion*, **59**, No. 7, 073001 (2019). https://doi.org/10.1088/1741-4326/ab2005

3. G. S. Nusinovich, M. K. A. Thumm, and M. I. Petelin, *J. Infrared Millim. Terahertz Waves*, **35**, 325–381 (2014). https://doi.org/10.1007/s10762-014-0050-7

4. M. Yu. Glyavin, A. G. Luchinin, and G. Yu. Golubiatnikov, *Phys. Rev. Lett.*, **100**, 015101 (2008). https://doi.org/10.1103/PhysRevLett.100.015101

5. V. L. Bratman, Yu. K. Kalynov, and V. N. Manuilov, *Phys. Rev. Lett.*, **102**, 245101 (2009). https://doi.org/10.1103/PhysRevLett.102.245101

6. A. V. Arzhannikov and S. L. Sinitsky, *Kiloampere Electron Beams for Vaccumm Oscillation Pumping in Plasmas* [in Russian], Publishing and Printing Center of the Novisibirsk State University (2016).

7. A. V. Arzhannikov, N. S. Ginzburg, P. V. Kalinin, et al., *Phys. Rev. Lett.*, **117**, No. 11, 114801 (2016). https://doi.org/10.1103/PhysRevLett.117.114801

8. N. S. Ginzburg, N. Yu. Peskov, and A. S. Sergeev, *Pis'ma Zh. Tekh. Fiz.*, **18**, No. 9, 23–28 (1992).

9. N. S. Ginzburg, N. Yu. Peskov, A. S. Sergeev, et al., *Izv. VUZ Appl. Nonlin. Dyn.*, **28**, No. 6, 575–632 (2020). https://doi.org/10.18500/0869-6632-2020-28-6-575-632

10. N. Yu. Peskov, E. D. Egorova, A. S. Sergeev, and I. M. Tsarkov, *Tech. Phys. Lett.*, **49**, No. 4, 57–61 (2023). https://doi.org/10.21883/TPL.2023.04.55880.19375

11. N. S. Ginzburg, V. Yu. Zaslavsky, I. V. Zotova, et al., *JETP Lett.*, **91**, No. 6, 266–270 (2010). https://doi.org/10.1134/S0021364010060020

12. N. Yu. Peskov, M. S. Ginzburg, I. I. Golubev, et al., *Appl. Phys. Lett.*, **116**, 213505 (2020). https://doi.org/10.1063/5.0006047

13. N. F. Kovalev, I. M. Orlova, and M. I. Petelin, *Radiophys. Quantum Electron.*, **11**, No. 5, 449–450 (1968). https://doi.org/10.1007/BF01034380

14. H. Kogelnik and C. V. Shank, *J. Appl. Phys.*, **43**, 2327–2335 (1972). https://doi.org/10.1063/1.1661499

15. A. Yariv, *Quantum Electronics*, John Wiley and Sons Inc., New York (1975).

16. N. S. Ginzburg and N. Yu. Peskov, *Phys. Rev. ST Accel. Beams*, **16**, 090701 (2013). https://doi.org/10.1103/PhysRevSTAB.16.090701

17. N. S. Ginzburg, N. A. Zavol'sky, G. S. Nusinovich, and A. S. Sergeev, *Radiophys. Quantum Electron.*, **29**, No. 1, 89–97 (1986). https://doi.org/10.1007/BF01034008

18. J. Benford, J. Swegle, and E. Shamiloglu, *High Power Microwaves*, Taylor & Francis, Boca Raton (2007).